

Direct Spectroscopic Observation of Intramolecular Hydrogen Shifts in Carbenes

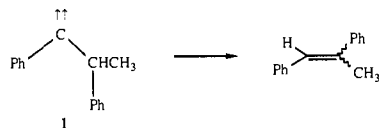
Robert J. McMahon and Orville L. Chapman*

Contribution from the Department of Chemistry and Biochemistry, University of California, Los Angeles, Los Angeles, California 90024. Received June 26, 1985

Abstract: Triplet *o*-tolylmethylene (**13a**) decays thermally to singlet *o*-xylylene (**14a**) in an argon matrix at temperatures as low as 4.6 K. The thermal, intramolecular [1,4]-hydrogen shift has been observed directly by IR and UV spectroscopy. The carbene disappearance kinetics follow the standard (time)^{1/2} dependence, due to multiple reaction sites in the matrix. The small temperature dependence and non-Arrhenius behavior of the rate implicate a tunneling mechanism. In contrast, triplet 1-phenylethylidene (**17a**) is thermally stable in argon or xenon matrices at 10 K. Warming **17a** to 65 K in a xenon matrix produces styrene (**18a**). The intramolecular [1,2]-hydrogen shift has been observed directly by IR spectroscopy. The carbene disappearance kinetics show apparent first-order behavior. We estimate an upper limit of ca 4.7 kcal/mol for the singlet-triplet energy gap in **17a**.

Intramolecular hydrogen migrations are among the common reactions of carbenes. Considerable theoretical¹ and experimental^{2,3} attention has focused on the activation energies,¹ geometrical requirements (orientation),^{1,2} and spin multiplicities³ involved in such processes. Despite the current interest in carbene reaction dynamics,⁴ however, the tremendously facile nature of intramolecular hydrogen shifts makes direct experimental studies difficult.

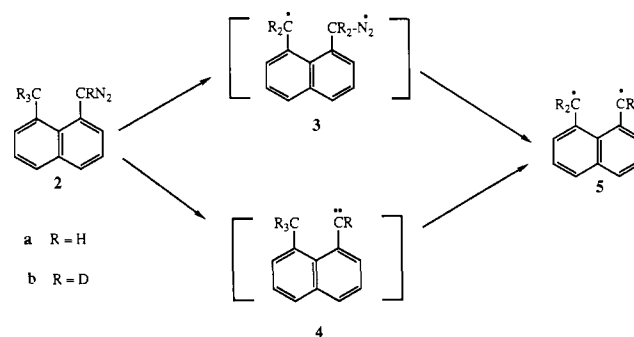
The literature contains few reports in this area. Tomioka and Platz,⁵ using ESR spectroscopy, examined the thermal [1,2]-hydrogen migration in triplet 1,2-diphenylpropylidene (**1**). Matrix effects prevented straightforward interpretation of the kinetic data. Platz and co-workers observed only the triplet biradical **5a** upon



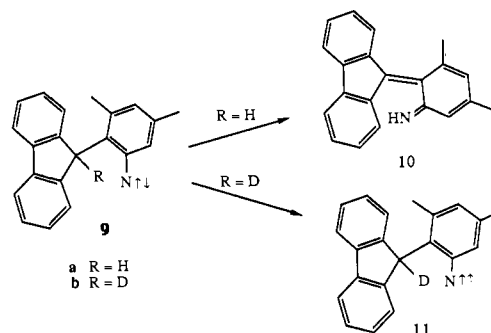
photolysis of 8-methyl-1-naphthylidiazomethane (**2a**) at 4.2 K (Scheme I).⁶ Surprisingly, even deuteration did not stop the migration. The decay of arylcarbenes in organic glasses, a reaction closely related to intramolecular hydrogen shifts, occurs by a tunneling mechanism.⁷

One might expect nitrenes to display reactivity similar to their isoelectronic carbene analogues. This has not been true in the systems studied thus far. Platz observed both nitrene **7** and

Scheme I



Scheme II



(1) Schaefer, H. F. *Acc. Chem. Res.* **1979**, *12*, 288-296. Frenking, G.; Schmidt, J. *Tetrahedron* **1984**, *40*, 2123-2132.

(2) Nickon, A.; Bronfenbrenner, J. K. *J. Am. Chem. Soc.* **1982**, *104*, 2022-2023. Tomioka, H.; Ueda, H.; Kondo, S.; Izawa, Y. *J. Am. Chem. Soc.* **1980**, *102*, 7818-7820. Press, L. S.; Shechter, H. *J. Am. Chem. Soc.* **1979**, *101*, 509-510. Dellacolella, B. A.; Shechter, H. *Tetrahedron Lett.* **1979**, 4817-4820. Kyba, E. P.; John, A. M. *J. Am. Chem. Soc.* **1977**, *99*, 8329-8330. Kyba, E. P. *J. Am. Chem. Soc.* **1977**, *99*, 8330-8332. Seghers, L.; Shechter, H. *Tetrahedron Lett.* **1976**, 1943-1946. Nickon, A.; Huang, F.; Weglein, R.; Matsuo, K.; Yagi, H. *J. Am. Chem. Soc.* **1974**, *96*, 5264-5265. Yamamoto, Y.; Moritani, I. *Tetrahedron* **1970**, *26*, 1235-1242.

(3) Fukushima, M.; Jones, M.; Brinker, U. H. *Tetrahedron Lett.* **1982**, *23*, 3211-3214. Kraska, A. R.; Chang, K.-T.; Chang, S.-J.; Moseley, C. G.; Shechter, H. *Tetrahedron Lett.* **1982**, *23*, 1627-1630. Chang, K.-T.; Shechter, H. *J. Am. Chem. Soc.* **1979**, *101*, 5082-5084.

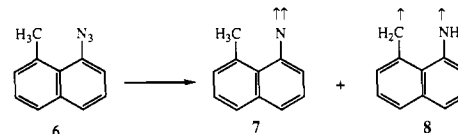
(4) Eisenthal, K. B.; Moss, R. A.; Turro, N. J. *Science* **1984**, 1439-1445. Simon, J. D.; Peters, K. S. *Acc. Chem. Res.* **1984**, *17*, 277-283. Griller, D.; Nazran, A. S.; Scaiano, J. C. *Acc. Chem. Res.* **1984**, *17*, 283-289.

(5) Tomioka, H.; Hayashi, N.; Izawa, Y.; Senthilnathan, V. P.; Platz, M. S. *J. Am. Chem. Soc.* **1983**, *105*, 5053-5057.

(6) Platz, M. S.; Carrol, G.; Pierrat, F.; Zayas, J.; Auster, S. *Tetrahedron* **1982**, *38*, 777-785. Platz, M. S. *J. Am. Chem. Soc.* **1980**, *102*, 1192-1194. Platz, M. S.; Burns, J. R. *J. Am. Chem. Soc.* **1979**, *101*, 4425-4426. Platz, M. S. *J. Am. Chem. Soc.* **1979**, *101*, 3398-3399. Fritz, M. J.; Ramos, E. L.; Platz, M. S. *J. Org. Chem.* **1985**, *50*, 3522-3526.

(7) Senthilnathan, V. P.; Platz, M. S. *J. Am. Chem. Soc.* **1980**, *102*, 7637-7643. Platz, M. S.; Senthilnathan, V. P.; Wright, B. B.; McCurdy, C. W. *J. Am. Chem. Soc.* **1982**, *104*, 6494-6501. Savino, T. G.; Soundararajan, N.; Platz, M. S. *J. Phys. Chem.* **1986**, *90*, 919-923.

biradical **8** upon photolysis of 1-azido-8-methylnaphthalene (**6**).⁶ Nitrene **7** does not produce **8** either thermally or photochemically.



Iwamura could not characterize the protium-substituted nitrene **11a** by ESR spectroscopy at 4.2 K due to the facile hydrogen shift⁸ (Scheme II). He did observe the deuterium-substituted nitrene **11b**, however. He concluded that [1,4]-hydrogen migration in singlet **9a** is faster than intersystem crossing to **11a**.

We now report direct, spectroscopic studies of intramolecular hydrogen shifts in carbenes. Our investigation of the tolylmethylene rearrangements provided intriguing examples of both [1,2]- and [1,4]-hydrogen shifts.⁹ We explore here the dynamics

(8) Murata, S.; Sugawara, T.; Iwamura, H. *J. Am. Chem. Soc.* **1983**, *105*, 3723-3724. Sugawara, T.; Nakashima, N.; Yoshihara, K.; Iwamura, H. *J. Am. Chem. Soc.* **1983**, *105*, 858-862. Murata, S.; Sugawara, T.; Iwamura, H. *J. Am. Chem. Soc.* **1985**, *107*, 6317-6329.

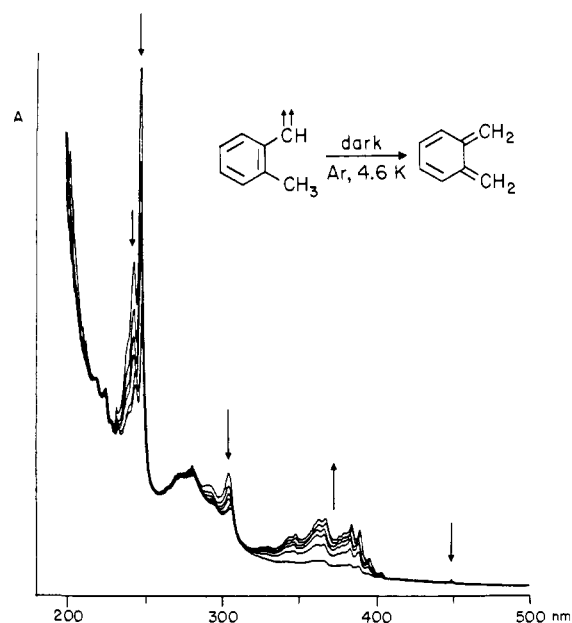


Figure 1. UV-visible spectra showing the decrease of *o*-tolylmethylene (**13a**) and concomitant increase of *o*-xylene (**14a**) upon standing in the dark at 12 K.

of the thermal [1,2]-hydrogen migration in 1-phenylethylidene (**17a**) that produces styrene (**18a**). The strong temperature dependence of the rearrangement enables us to turn this facile reaction "off" at sufficiently low temperatures ($T < 35$ K). In striking contrast, the thermal [1,4]-hydrogen shift in *triplet o*-tolylmethylene (**13a**) that produces *singlet o*-xylene (**14a**) occurs at temperatures as low as 4.6 K.

Results

***o*-Tolyldiazomethane (12a).** We examined the photochemistry of *o*-tolyldiazomethane (**12a**) under three different types of irradiation conditions.

(1) Long-wavelength irradiation (>470 nm) of argon-matrix-isolated **2a** produces *triplet o*-tolylmethylene (**13a**: UV, (Ar, 15 K) λ_{\max} 450, 440, 437, 435, 431, 427, 422, 419, 417, 413, 305, 292, 249, and 244 nm; ESR, (Ar, 20 K), major rotomer $|D/hc| = 0.503$ cm $^{-1}$, $|E/hc| = 0.0253$ cm $^{-1}$, $Z_1 = 2055$ G, $X_2 = 4839$ G, $Y_2 = 5879$ G, $Z_2 = 8679$ G, microwave frequency 9.263 GHz, minor rotomer $|D/hc| = 0.503$ cm $^{-1}$, $|E/hc| = 0.0244$ cm $^{-1}$, $Z_1 = 2055$ G, $X_2 = 4900$ G, $Y_2 = 5826$ G, $Z_2 = 8679$ G, microwave frequency 9.263 GHz) and *o*-xylene (**14a**: UV, (Ar, 15 K) λ_{\max} 403, 395, 389, 384, 379, 376, 367, 362, 347, 342, 329, and 326 nm; IR (Ar, 15 K) 1575 w, 1548 m, 1493 m, 1469 w, 869 s, 774 m, 754 m, 635 m, and 436 w cm $^{-1}$). The structural assignment of *o*-xylene (**14a**) rests on comparison of the IR and UV spectra with those reported in the literature.¹⁰ Under these irradiation conditions, no IR bands could be attributed to *o*-tolylmethylene (**13a**), and 1-methylcycloheptatetraene (**15a**) was not observed. The UV absorptions of carbene **13a** reach a maximum after ca. 25 h of irradiation. Continued photolysis (>470 nm) for up to 86 h results only in a *decrease* in the absorptions, even though the longest wavelength maximum of **13a** lies at 450 nm. Irradiation (>416 nm) leads to the rapid and irreversible disappearance of the ESR and UV signals of carbene **13a**.

(2) Irradiation (>416 nm, 1300 min) of **12a**, matrix isolated in argon, produces *o*-xylene (**14a**: IR vide supra) and 1-methylcycloheptatetraene (**15a**: IR (Ar, 15 K) 1386 m, 790 s, 710 s, 655 m, 588 m, and 503 w cm $^{-1}$) in a roughly 2:1 ratio, as observed by IR spectroscopy.

(3) Flash irradiation (>200 nm, 1.0 min) of a thin argon matrix containing *o*-tolyldiazomethane (**12a**) gives high conversion to

Table I. First-Order Rate Constants for *o*-Tolylmethylene Disappearance in Argon at 20 K by ESR Spectroscopy

transition	experiment 1 rate $\times 10^6$ s $^{-1}$	experiment 2 rate $\times 10^6$ s $^{-1}$
Z_1	2.7	4.3
X_2	3.5	6.4
Y_2	2.9	5.5
Z_2		

Table II. First-Order Rate Constants for *o*-Tolylmethylene Disappearance in Argon by UV Spectroscopy

temp (K)	experiment 1 rate $\times 10^6$ s $^{-1}$	experiment 2 rate $\times 10^6$ s $^{-1}$
4.6	3.2	3.1
5.8	3.9	2.9
8.1	3.7	3.1
12.0	3.9	2.9
18.0	4.9	3.7
25.0	4.0	3.5
30.0	4.0	4.6

Table III. First-Order Rate Constants for *o*-Tolylmethylene Disappearance in Xenon at 12 K by UV Spectroscopy

absorption	experiment 1 rate $\times 10^6$ s $^{-1}$	experiment 2 rate $\times 10^6$ s $^{-1}$
244 nm	1.8	1.1
249 nm	2.3	1.3

triplet o-tolylmethylene (**13a**: IR (Ar, 10 K) 742 cm $^{-1}$; UV and ESR vide supra). IR and UV studies show that small amounts of *o*-xylene (**14a**) and 1-methylcycloheptatetraene (**15a**) are also formed.

The UV experiment described in part 1 suggests that *triplet o*-tolylmethylene (**13a**) is thermally unstable (even at 15 K) and decays to *o*-xylene (**14a**). We therefore generated carbene **13a** photochemically and monitored its thermal disappearance spectroscopically (IR, UV,¹¹ ESR;¹² Figures 1 and 2). The kinetics of the process were analyzed in terms of the usual (time)^{1/2} dependence for solid-state reactions (short-irradiation-time limit) (Figure 3). Neither first-order nor second-order kinetics fit the data well. Intermolecular solid-state reactions such as carbene decay,⁷ radical decay,¹³ and energy transfer¹⁴ generally exhibit a $t^{1/2}$ dependence due to multiple reaction sites in the solid host. Doba, Ingold, and Siebrand showed how to extract meaningful rate constants from $t^{1/2}$ plots.¹⁵

The data in Table I establish that the Z_1 , X_2 , and Y_2 ESR transitions of **13a** disappear at the same rate, within experimental error (ca. $\pm 1.5 \times 10^{-6}$ s $^{-1}$). The reproducibility of the rate constants is definitely better than an order of magnitude. The data also demonstrate that the major rotomer decays much more rapidly than the minor rotomer.

The UV spectrum of **13a** consists of a superposition of the absorptions of both rotomers. Since the minor rotomer is present in low concentration and decays relatively slowly, the experimental rate constants closely approximate the decay rate of the major rotomer (Table II). For this reason, the rate constants for ESR and UV disappearance of **13a** agree quite well. The UV rate

(11) In the UV-vis experiment, carbene **13a** was generated by $\lambda > 200$ nm irradiation. We plotted the natural logarithm of the peak area vs. (time)^{1/2}. Peak areas of UV absorptions were integrated with use of Perkin-Elmer Corp. PECUV spectroscopy software. Peak heights were not used, as base line changes (due to matrix degradation) occur at temperatures above ca. 25 K.

(12) In the ESR experiment, carbene **13a** was generated by $\lambda > 470$ nm irradiation. We plotted the natural logarithm of the height of the ESR transition vs. (time)^{1/2}. The magnet and microwave bridge were turned off, except while spectra were being recorded.

(13) Doba, T.; Ingold, K. U.; Siebrand, W.; Wildman, T. A. *J. Phys. Chem.* **1984**, *88*, 3165-3167 and references therein.

(14) Forster, T. *Mod. Quantum Chem.* **1965**, *3*, 93. Yardley, J. T. *Introduction to Molecular Energy Transfer*; Academic: New York, 1980; p 234.

(15) Doba, T.; Ingold, K. U.; Siebrand, W. *Chem. Phys. Lett.* **1984**, *103*, 339-342. Siebrand, W.; Wildman, T. A. *Acc. Chem. Res.* **1986**, *19*, 238-243.

(9) Chapman, O. L.; McMahon, R. J.; West, P. R. *J. Am. Chem. Soc.* **1984**, *106*, 7973-7974.

(10) Tseng, K. L.; Michl, J. *J. Am. Chem. Soc.* **1977**, *99*, 4840-4842.

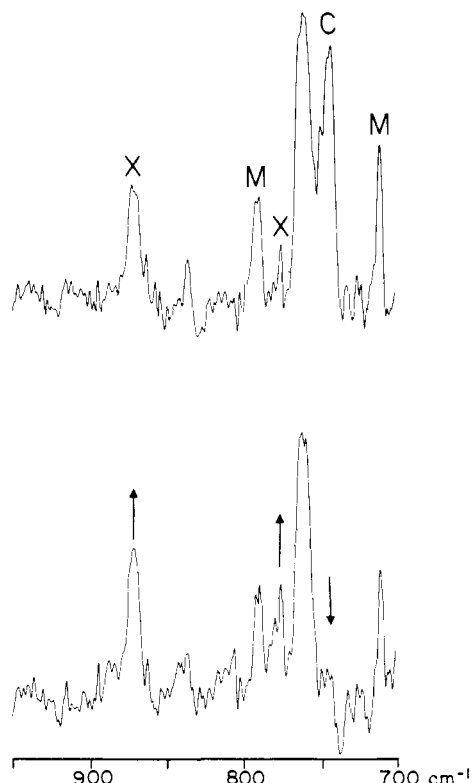


Figure 2. Top: Infrared spectrum (in absorbance) showing the mixture of *o*-tolylmethylene (C), *o*-xylylene (X), and 1-methylcycloheptatriene (M) obtained upon irradiation (>200 nm, 1.0 min) of *o*-tolyl diazomethane matrix isolated in argon at 10 K. Bottom: Spectrum showing disappearance of *o*-tolylmethylene with concomitant increase of *o*-xylylene upon standing in the dark at 10 K for 3.25 h.

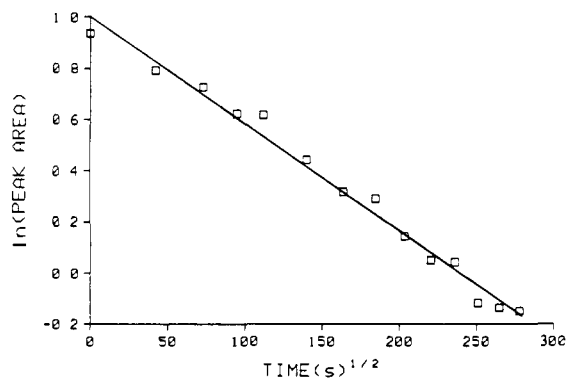


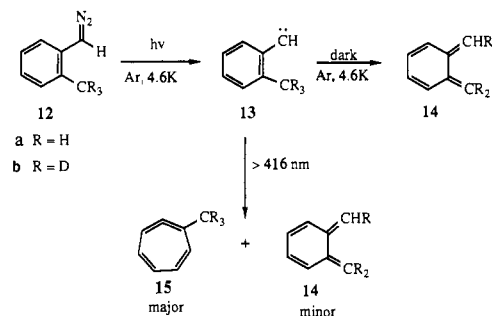
Figure 3. Kinetic plot of the decrease of the 249-nm UV absorption of argon-matrix-isolated *o*-tolylmethylene (**13a**) upon standing in the dark at 12 K.

constants clearly possess smaller error limits (ca. $\pm 0.7 \times 10^{-6} \text{ s}^{-1}$). The UV-disappearance rates are slightly slower in xenon (Table III), although the difference lies barely beyond the error limits. We conclude that xenon has but a small effect on the rate of reaction.

Although we observed the thermal conversion of carbene **13a** to *o*-xylylene (**14a**) by IR spectroscopy (Figure 2), disappearance rates could not be measured. We were unable to accurately integrate such weak absorptions. IR and UV spectroscopy clearly establish *o*-xylylene (**14a**) growth concomitant with *o*-tolylmethylene (**13a**) disappearance. We are unable, however, to monitor the reaction for enough half-lives to obtain an accurate "infinity" concentration of *o*-xylylene (**14a**). Appearance rate constants are very sensitive to the "infinity" concentration. We are therefore unable to analyze the kinetics of *o*-xylylene appearance.

***o*-(Trideuteriomethyl)phenyldiazomethane (12b).** Irradiation (>470 nm) of argon-matrix-isolated **12b** produces triplet *o*-(tri-

Scheme III



deuteriomethyl)phenylmethylene (**13b**: IR (Ar, 15 K) 3070 m, 2240 w, 1041 w, 747 m, 739 s, 669 m, and 442 w cm^{-1} ; UV (Ar, 15 K) λ_{max} 449, 440, 431, 417, 414, 299, 245, and 241 nm; ESR (Ar, 19 K) major rotomer $|D/hc| = 0.521 \text{ cm}^{-1}$, $|E/hc| = 0.0246 \text{ cm}^{-1}$, $Z_1 = 2256 \text{ G}$, $X_2 = 4894 \text{ G}$, $Y_2 = 5920 \text{ G}$, $Z_2 = 8852 \text{ G}$; microwave frequency 9.266 GHz; minor rotomer $|D/hc| = 0.505 \text{ cm}^{-1}$, $|E/hc| = 0.0246 \text{ cm}^{-1}$, $Z_1 = 2070 \text{ G}$, $X_2 = 4856 \text{ G}$, $Y_2 = 5873 \text{ G}$, $Z_2 = 8687 \text{ G}$, microwave frequency 9.266 GHz). Irradiation (>420 nm) destroys the IR, UV, and ESR signals of *o*-(trideuteriomethyl)phenylmethylene (**13b**) and generates 1-(trideuteriomethyl)cycloheptatriene (**15b**, major product) and trideuterio-*o*-xylylene (**14b**, minor product).¹⁶

The thermal stability of **13b** is demonstrated by its generation upon long-wavelength irradiation (>470 nm, 3900 min) of **12b**. This contrasts with the protio-analogue **13a**, which decays during the lengthy photolysis. Furthermore, the UV and ESR signals do not decay upon standing in the dark in argon at 19 K. Preliminary results indicate that trideuteriomethyl carbene **13b** is quite stable at higher temperatures as well. Irradiation (>470 nm) of **12b** matrix isolated in xenon at 23 K generates carbene **13b**. Warming to 59 K produces a matrix that severely scatters visible light. The carbene **13b** is barely discernable in the noisy spectrum, but the signal does not change appreciably upon standing at 59 K for 1150 min. Subsequent irradiation of the matrix under conditions known to destroy carbene **13b** (>420 nm, 64 min) destroys the UV absorption, thereby confirming the carbene assignment.

1-Phenyldiazoethane (16a) in Argon. Irradiation (>470 nm) of argon-matrix-isolated 1-phenyldiazoethane (**16a**) produces triplet 1-phenylethylidene (**17a**: IR (Ar, 15 K) 3090 w, 3075 m, 3038 w, 2942 w, 2920 w, 2893 w, 2862 m, 2807 w, 2690 vw, 1468 m, 1018 m, 1007 w, 875 w, 740 s, 670 s, and 480 m cm^{-1} ; UV (Ar, 15 K) λ_{max} 449, 446, 432, 428, 417, 412, 405, 399, 392, 388, 381, 302, 251, and 244 nm; ESR: (Ar, 15 K) $|D/hc| = 0.508 \text{ cm}^{-1}$, $|E/hc| = 0.0279 \text{ cm}^{-1}$, $Z_1 = 2100 \text{ G}$, $X_2 = 4784 \text{ G}$, $Y_2 = 5937 \text{ G}$, $Z_2 = 8734 \text{ G}$, microwave frequency 9.313 GHz) and a small amount of styrene (**18a**: IR vide infra). Neither prolonged irradiation (>470 nm), nor standing at 12 K (14 h), nor warming to 36 K results in a change in the infrared spectrum of the products. Irradiation (>440 nm) leads to the disappearance of the IR, UV, and ESR signals of **17a** and to the appearance of styrene (**18a**: IR (Ar, 15 K) 3115 vw, 3095 m, 3070 m, 3035 m, 3000 vw, 1960 vw, 1942 vw, 1889 vw, 1872 vw, 1811 w, 1800 vw, 1746 vw, 1690 vw, 1637 m, 1603 w, 1581 w, 1499 m, 1456 m, 1431 w, 1415 w, 1338 w, 1320 w, 1295 w, 1262 vw, 1208 w, 1182 vw, 1103 vw, 1084 m, 1022 m, 994 m, 980 w, 905 s, 780 s, 698 s, 552 m, and 433 m cm^{-1} ; UV (Ar, 15 K) 288, 280, 278, 271, 255, 245, 237, and 211 nm). Irradiation (>470 nm) of 1-phenyldiazoethane (**16a**) in a carbon monoxide doped argon matrix generates 1-phenylethylidene (**17a**: IR vide supra) and a trace of ketene **19** (2110 cm^{-1}). Warming the matrix to 39 K (30 min) results in the decrease in intensity of the IR bands of **17a** and CO (2139 cm^{-1}) and in the increase in intensity of the IR bands of

(16) The detailed structural assignments for these species will be presented in the full paper concerning the tolylmethylene rearrangements. Chapman, O. L.; Johnson, J. W.; McMahon, R. J.; West, P. R. submitted to *J. Am. Chem. Soc.*

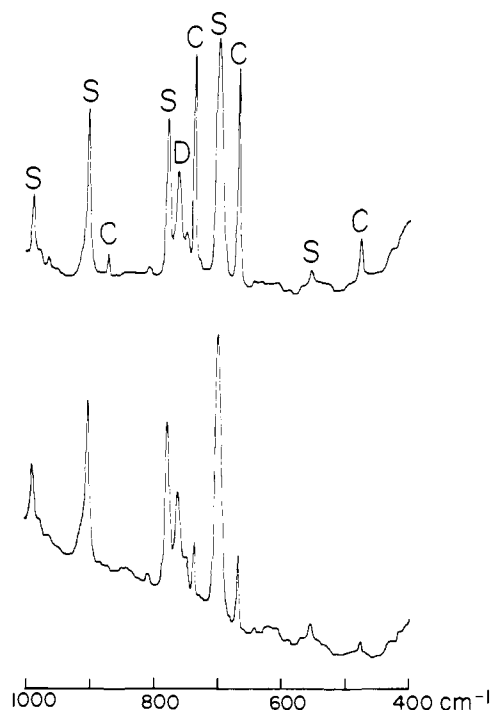
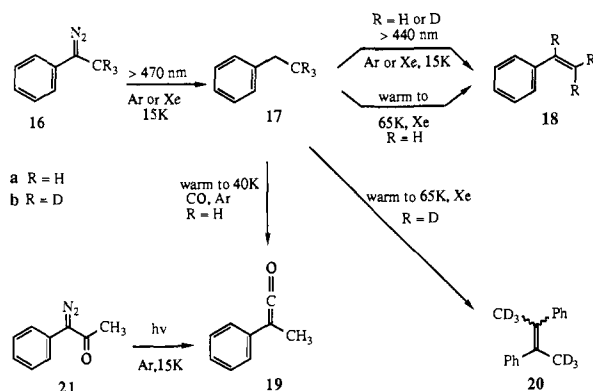


Figure 4. Top: Infrared spectrum (in absorbance) of 1-phenylethylidene (**17a**) matrix isolated in xenon immediately after warming to 65 K. Substantial increase in styrene (**18a**) intensity and decrease in carbene (**17a**) intensity has already occurred during the warming process. Bottom: Infrared spectrum (in absorbance) showing carbene (**17a**) disappearance and styrene (**18a**) appearance upon standing at 65 K for 78 min. C = carbene, S = styrene, D = dimer.

Scheme IV



ketene **19**. The identity of ketene **19** was established by comparison of the IR spectrum with that of the material prepared by irradiation (>336 nm) of 1-diazo-1-phenyl-2-propanone (**21**) (IR vide infra) (Scheme IV).

1-Phenyldiazoethane (16a) in Xenon. We examined the thermal stability of 1-phenylethylidene (**17a**) in xenon matrices. The useful temperature range of xenon matrices extends to ca. 80 K. Irradiation (>470 nm) of xenon-matrix-isolated 1-phenyldiazoethane (**16a**) produces triplet 1-phenylethylidene (**17a**), along with small amounts of styrene (**18a**) and dimer (Figure 4). The UV absorptions of **16a**, **17a**, and **18a** are each red-shifted 5–8 nm relative to their positions in argon. In contrast to the argon studies, infrared spectroscopy reveals that prolonged irradiation (>470 nm) results in a slow decrease in carbene **17a** intensity and an increase in styrene (**18a**) intensity. The infrared spectrum of the products, however, does not change upon standing in the dark at 12 K (24 h). Irradiation (>416 nm) of **17a** rapidly produces styrene (**18a**), as monitored by UV spectroscopy.

Increasing the temperature of a xenon matrix of 1-phenylethylidene (**17a**) from 12 to 35 K results in a small, rapid decrease in carbene (**17a**) concentration and an increase in styrene (**18a**)

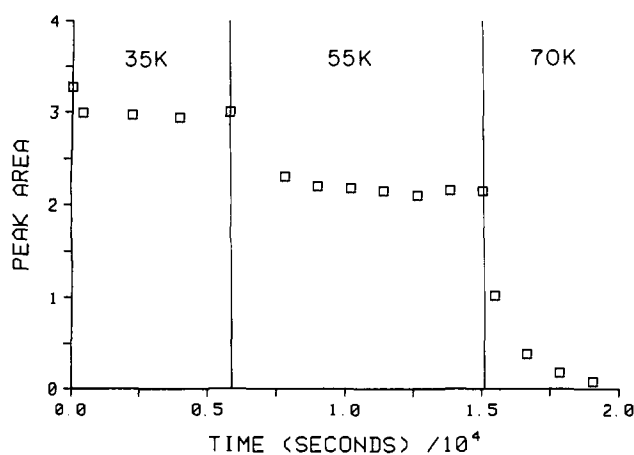


Figure 5. Plot of intensity of the 740-cm⁻¹ IR absorption of xenon-matrix-isolated 1-phenylethylidene (**17a**) vs. time. Site-clearing behavior is observed at various temperatures.

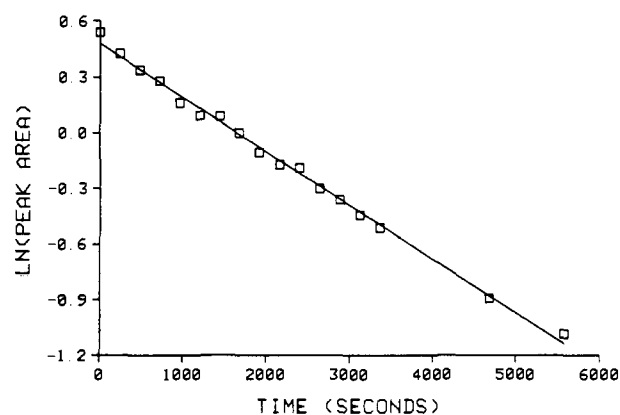


Figure 6. First-order kinetic plot for disappearance of the 740-cm⁻¹ band of 1-phenylethylidene (**17a**) in xenon at 65 K. Least-squares fit gives $k_{\text{disappear}} = 2.9 \times 10^{-4} \text{ s}^{-1}$ ($R = 0.998$).

concentration, as monitored by IR spectroscopy. Almost no change occurs once the temperature stabilizes at 35 K (Figure 5). Warming from 35 to 55 K produces similar behavior, but warming from 55 to 75 K produces smooth disappearance of carbene **17a** and growth of styrene (**18a**) (Figure 5). Throughout this process, dimer concentration does not change detectably. After xenon-matrix-isolated 1-phenylethylidene (**17a**) was warmed from 12 to 65 K, carbene disappearance and styrene appearance were monitored by infrared spectroscopy (Figure 4).¹⁷ Carbene **17a** disappearance obeys first-order kinetics ($k_{\text{disappear}} = 2.9 \times 10^{-4} \text{ s}^{-1}$) (Figure 6). In this instance, neither $(\text{time})^{1/2}$ dependence nor second-order kinetics fit the data well. A $t^{1/2}$ dependence is normally obeyed in solid-state reactions with multiple reaction sites.^{7,13-15} With a severe distribution of reaction sites, a $t^{1/3}$ dependence is required.⁷ The apparent first-order dependence (t^1), rather than a $t^{1/2}$ dependence, reflects the absence of a severe multiple-site problem in xenon at 65 K. Xenon is extremely soft at 65 K.

Warming the xenon matrix produces styrene (**18a**) as the sole product (IR). At lower xenon:substrate ratios, or at higher temperatures where the xenon matrix degrades more rapidly, dimer formation occurs, and carbene (**13a**) disappearance obeys second-order kinetics. Under conditions of good matrix isolation at 65 K, second-order dimerization is much slower than first-order styrene (**18a**) formation.

As with the case of *o*-xyllylene (**14a**) appearance discussed before, we can monitor styrene (**18a**) appearance, but we cannot analyze the kinetic data. We are unable to obtain an accurate "infinity" reading of styrene (**18a**) concentration due to matrix

(17) Peak areas of infrared absorptions were integrated with use of Perkin-Elmer Corp. PECDs II infrared spectroscopy software.

degradation. We were unable to monitor carbene disappearance by ESR spectroscopy because we could not consistently maintain a xenon matrix at 65 K on our ESR cryostat tip. Even when the matrix remained intact at this temperature, the weak signal precluded accurate kinetic analysis. We could not monitor carbene disappearance by UV spectroscopy. The UV absorptions of carbene **17a** and styrene (**18a**) strongly overlap. The $\pi-\pi^*$ visible absorptions of **17a** are too weak to integrate accurately. We were unable to measure the temperature dependence; the temperature at which the rate becomes conveniently measurable (65 K) lies near the upper limit of the useful range of a xenon matrix.

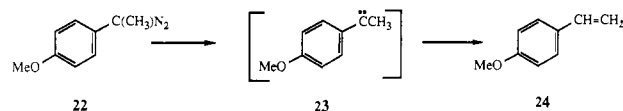
2,2,2-Trideuterio-1-phenyldiazoethane (16b) in Argon. Irradiation (>470 nm) of 2,2,2-trideuterio-1-phenyldiazoethane (**16b**) produces triplet 2,2,2-trideuterio-1-phenylethylidene (**17b**: IR (Ar, 15 K) 2179 w, 2095 w, 2079 w, 1468 m, 1432 w, 1424 w, 1181 w, 1172 w, 1090 w, 1060 w, 1033 m, 1019 w, 947 m, 878 m, 862 w, 736 s, 670 s, and 475 m cm^{-1} ; UV (Ar, 25 K) λ_{max} 449 sh, 446, 432, 428, 420, 416, 411, 404, 400, 303, 251, 245, and 203 nm; ESR (Ar, 15 K) $|D/hc| = 0.511 \text{ cm}^{-1}$, $|E/hc| = 0.0285 \text{ cm}^{-1}$, $Z_1 = 2138 \text{ G}$, $X_2 = 4775 \text{ G}$, $Y_2 = 5960 \text{ G}$, $Z_2 = 8763 \text{ G}$, microwave frequency 9.264 GHz) and a small amount of α,β,β -trideuteriostyrene (**18b**: IR wide infra). Irradiation (>416 nm) of 2,2,2-trideuterio-1-phenylethylidene (**17b**) rapidly produces α,β,β -trideuteriostyrene (**18b**: IR (Ar, 15 K) 3110 w, 3095 m, 3070 m, 3030 m, 2258 w, 2220 w, 1601 s, 1568 m, 1497 m, 1449 m, 1180 w, 1092 w, 1081 w, 1049 w, 1044 w, 1019 w, 1004 w, 911 w, 833 w, 790 m, 743 s, 710 s, 690 s, 582 w, 570 w, 562 w, 548 w, 508 m, 408 w, and 397 w cm^{-1} ; UV (Ar, 15 K) 290, 286, 281, 278, 275, 270, 256, 247, 239, and 211 nm). The trideuteriostyrene (**18b**) assignment is based on comparison of the IR and UV spectra with those of styrene (**18a**). The UV spectra are virtually identical, and the IR spectra exhibit striking similarities.

2,2,2-Trideuterio-1-phenyldiazoethane (16b) in Xenon. As with the protio compound, we studied the thermal stability of 2,2,2-trideuterio-1-phenylethylidene (**17b**) in xenon matrices. Irradiation of xenon-matrix-isolated 2,2,2-trideuterio-1-phenyldiazoethane (**16b**) produces triplet 2,2,2-trideuterio-1-phenylethylidene (**17b**), along with small amounts of trideuteriostyrene (**18b**) and dimer. The UV absorptions of **16b**, **17b**, and **18b** are each red-shifted 5–8 nm relative to their positions in argon. Xenon causes substantial broadening of the ESR signals of **17b**, relative to argon (150 G vs. 50 G full width at half maximum). The positions of the transitions are shifted, but the zero-field splitting parameters remain similar (ESR (Xe, 15 K) $|D/hc| = 0.516 \text{ cm}^{-1}$, $|E/hc| = 0.0270 \text{ cm}^{-1}$, $Z_1 = 1863 \text{ G}$, $X_2 = 4825 \text{ G}$, $Y_2 = 5950 \text{ G}$, $Z_2 = 8500 \text{ G}$, microwave frequency 9.262 GHz). In contrast to the argon studies, UV spectroscopy reveals that prolonged irradiation (>470 nm) results in a decrease in carbene **17b** intensity. Irradiation (>416 nm) of **17b** rapidly produces trideuteriostyrene (**18b**), as monitored by IR and UV spectroscopy.

After xenon-matrix-isolated 2,2,2-trideuterio-1-phenylethylidene (**17b**) is warmed from 12 to 80 K over 12 min, trideuteriocarbene (**17b**) and trideuteriostyrene (**18b**) concentrations were monitored by IR spectroscopy. Small changes occur during the warming. Remarkably, only a small amount of carbene disappears after 24 h at 80 K. No detectable increase in trideuteriostyrene (**18b**) concentration occurs. Such small changes in concentration over such long periods of time preclude any meaningful kinetic analysis. Recooling the matrix to 12 K followed by irradiation (>416 nm) rapidly destroys the carbene (**17b**) and produces trideuteriostyrene (**18b**). Similar experiments with UV monitoring of either the weak $\pi-\pi^*$ transitions (ca. 450 nm) or the aromatic transitions (ca. 250 nm) show the extremely slow disappearance of trideuteriocarbene **17b** in xenon at elevated temperatures. However, UV spectroscopy is not diagnostic in determining the structure of the products that form. Again, we could not obtain accurate kinetic data.

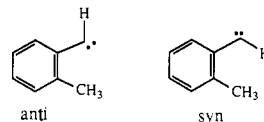
1-(4-Methoxyphenyl)diazoethane (22). Methoxy substitution increases the rate of [1,2]-hydrogen migration.¹⁸ We prepared 1-(4-methoxyphenyl)diazoethane (**22**) in an attempt to increase

the rate of the hydrogen shift in carbene **23**, relative to that in 1-phenylethylidene (**17a**). We hoped to monitor the reaction **23** \rightarrow **24** at lower temperatures in argon matrices. This would circumvent the problems associated with xenon matrices. Preliminary studies demonstrate that irradiation (>470 nm) of **22**, matrix isolated in argon at 15 K, produces *p*-methoxystyrene (**24**: IR (Ar, 15 K) 3100 w, 3020 w, 2965 w, 2945 w, 2915 w, 2843 m, 1630 m, 1612 m, 1580 w, 1513 s, 1465 m, 1459 w, 1442 w, 1428 w, 1413 w, 1321 m, 1304 m, 1291 m, 1258 s, 1250 s, 1183 m, 1175 s, 1115 w, 1052 m, 1048 m, 1029 w, 990 m, 895 m, 833 s, 818 w, 808 w, 712 w, 552 w, 527 w, and 493 s cm^{-1}). We do not know whether this is due to an extremely facile thermal rearrangement of carbene **23** or whether the UV absorption of **23** is shifted such that the rearrangement is a photochemical process.



Discussion

Carbene Characterization. Observation of triplet ESR signals for carbenes **13a**, **13b**, **17a**, and **17b** at 15 K implies that the triplet state is the ground state or lies within several cal/mol of the ground state¹⁹ as expected for arylcarbenes.²⁰ Although we initially reported no rotational isomerism in *o*-tolylmethylene (**13a**),⁹ reexamination of the ESR spectra reveals that a small amount of a second rotomer is reproducibly present. Annealing the matrix at 30 K for 90 min rules out a multiple-site problem as the cause for the two sets of ESR transitions. The structural assignment of the rotomers presents a tricky problem. Hutton and Roth reported that rotational isomerism in arylcarbenes may arise as a consequence of differing π -spin densities at the two ortho positions.²¹ In many instances, isomerism cannot be detected in systems without differing ortho spin densities.^{21,22} The methyl substituent in *o*-tolylmethylene (**13a**) will not perturb the spin density enough to cause isomerism. The observed rotational isomerism must result from a steric effect. Our assignment rests on the observation that the major rotomer of **13a** thermally decays more rapidly than the minor rotomer and the argument that the anti conformer is the more appropriate geometry for hydrogen migration. The trideuterio-analogue **13b** also shows rotational isomerism. The transitions of the major rotomer of **13a** fortuitously match the transitions of the minor rotomer of **13b**, but the minor rotomer of **13a** and the major rotomer of **13b** differ significantly. The major species in each case should correspond to the anti isomer. The ESR spectra of the ethylidenes **17a** and



17b are unexceptional. The zero-field splitting parameters of **17a** agree with the values reported in the literature,²³ but the transitions display unreported fine structure. This fine structure cannot be due to rotational isomerism. Annealing the matrix rules out a multiple-site effect. A carbon monoxide trapping study provided chemical evidence for the triplet carbene structure of **17a**. Warming **17a** in a CO-doped argon matrix produces ketene **19** (Scheme IV). We find this type of trapping study to be diagnostic

(19) Platz, M. S. In *Diradicals*; Borden, W. T., Ed.; Wiley: New York, 1982; p 208.

(20) (a) Kirmse, W. *Carbene Chemistry*, 2nd ed.; Academic: New York, 1971; Chapter 6. (b) Trozzolo, A. M.; Wasserman, E. In *Carbenes*; Moss, R. A., Jones, M., eds.; R. E. Kreiger: Malabar, FL, 1983; Vol. II, Chapter 5.

(21) Hutton, R. S.; Roth, H. D. *J. Am. Chem. Soc.* **1982**, *104*, 7395–7399. Roth, H. D.; Hutton, R. S. *Tetrahedron* **1985**, *41*, 1567–1578.

(22) *m*-Tolylmethylene is one example of this behavior.⁹
(23) Murray, R. W., unpublished results. Cited in: Wasserman, E.; Barash, L.; Yager, W. A. *J. Am. Chem. Soc.* **1965**, *87*, 4974–4975. No experimental details (temperature, matrix material, irradiation conditions, thermal stability) are reported.

(18) Liu, M. T. H.; Tencer, M. *Tetrahedron Lett.* **1983**, *24*, 5713–5714 and references therein.

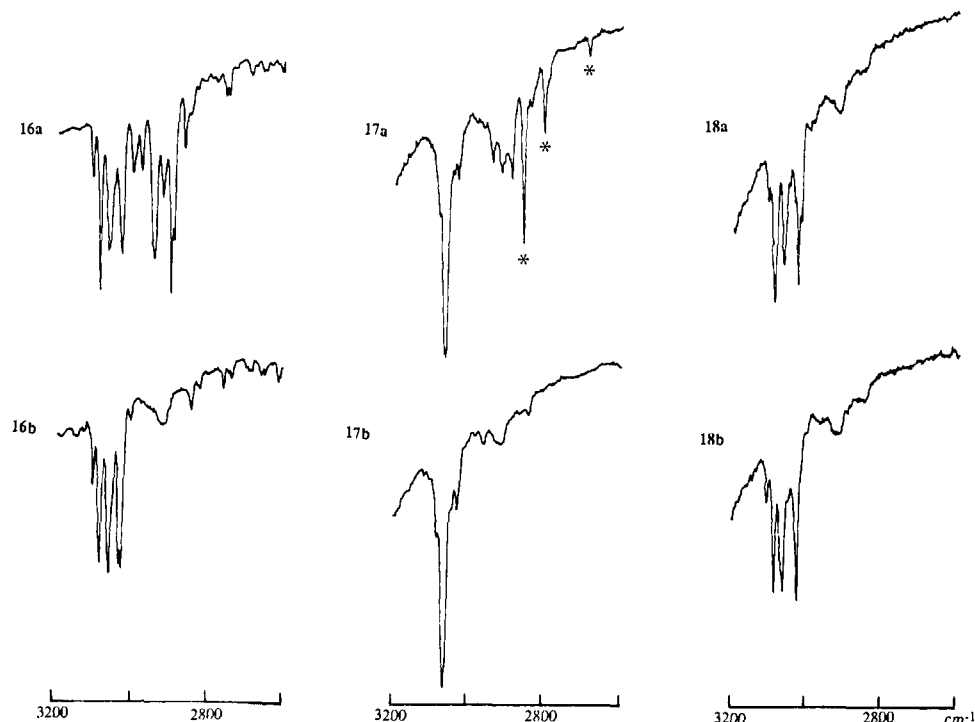


Figure 7. Infrared spectra (in transmittance) showing the C-H stretching vibrations of diazocompounds **16a** and **16b**, ethylenes **17a** and **17b**, and styrenes **18a** and **18b**. Bands marked with an asterisk (*) are fundamental C-H stretching modes of the methyl group adjacent to the triplet carbene center in **17a**.

for the presence of triplet carbenes.^{24,25}

The UV-visible spectra of **13a**, **13b**, **17a**, and **17b** provide strong confirmation of the triplet arylcarbene structural assignment. Each carbene displays the weak, long-wavelength $\pi-\pi^*$ transitions with extensive vibronic coupling characteristic of triplet arylcarbenes^{9,24-26} and the benzyl radical.²⁷ In addition, the carbenes each exhibit a weak absorption at 300–305 nm, and two strong, closely spaced absorptions at 240–250 nm. These bands have been observed previously in phenylmethylene.²⁴ The positions of the absorptions depend on the matrix; in xenon, the absorptions shift 5–8 nm to the red relative to argon.

The IR spectra of **13** and **17** indicate that these carbenes contain intact aromatic rings. As expected, the spectra of **13a** and **13b** are quite similar. The 1-phenylethylenes **17a** and **17b** both display the ca. 740, 670, and 480-cm⁻¹ bands characteristic of monosubstituted arylcarbenes. These bands have been observed previously in phenylmethylene and α -deuteriophenylmethylene.²⁴

The infrared spectrum of 1-phenylethylidene (**17a**) reveals the influence of the triplet carbene center on the C-H stretching modes of the adjacent methyl substituent. This is the first alkyl-substituted carbene to be observed by infrared spectroscopy. The IR spectrum of **17a** contains several bands in the aliphatic C-H stretching region (2944 w, 2920 w, 2895 w, 2860 m, 2840 vw, 2805 w, and 2685 vw cm⁻¹) (Figure 7). Warming **17a** to 36 K produced no change in the pattern or intensity of the C-H stretching vibrations. This suggests that, even at 15 K, methyl group rotation is fast on the infrared time scale. In a related open-shell system, *ab initio* calculations predict a 150-cal/mol barrier for the C-C rotation in the ethyl radical.²⁸ Pacansky was unable to freeze out this rotation in argon at 4 K.²⁹ The IR

spectrum of the trideuterio-analogue **17b** contains only three weak bands in the C-H stretching region (2965 vw, 2920 vw br, and 2845 vw cm⁻¹) (Figure 7). Styrene (**18a**), which also does not contain a methyl group, displays absorptions at 2920 w br and 2850 w br cm⁻¹. It is therefore likely that the 2944, 2920, 2895, and 2840-cm⁻¹ bands of **17a** are due to overtones or combinations, while the remaining absorptions (2860, 2805, and perhaps 2685 cm⁻¹) are due to fundamental C-H stretching vibrations of the methyl substituent. In support of this assignment, we note that these absorptions disappear as the methyl group is destroyed upon irradiation of the carbene to form styrene. For comparison, the C-H stretching modes in ethane occur at 2995, 2954, and 2950 cm⁻¹.²⁸ The rather low-frequency position of the methyl-group C-H stretching vibrations in **17a** indicates a weakening of the C-H bonds by the carbene center. This observation verifies the prediction of strong hyperconjugation in methylcarbene.³⁰ A radical center produces a similar, but less pronounced, effect on the β C-H bonds in the ethyl radical (3033, 2920, and 2842 cm⁻¹).²⁸ In an analogous manner, trideuteriocarbene **17b** exhibits weak vibrations at 2178, 2160, and 2080 cm⁻¹, a region in which **17a** displays no absorptions. We do not know which of these modes are fundamental C-D stretching vibrations. Again, we note a similarity between the IR absorptions of **17b** and the perdeuterioethyl radical (2199, 2098, and 2048 cm⁻¹).²⁸ Irradiation (>416 nm) destroys the alkyl C-D stretching modes of **17b** with concomitant appearance of the vinyl C-D stretching modes of trideuteriostyrene (**18b**) (2255, 2218 cm⁻¹).

[1,4]-Hydrogen Shift in *o*-Tolylmethylene (13a**).** The thermal rearrangement of triplet *o*-tolylmethylene (**13a**) to *o*-xylylene (**14a**) at 4.6 K strongly suggests a tunneling mechanism.³¹ The small temperature dependence of the rate and the nonlinear Arrhenius plot (*vide infra*) support this conclusion. Within the constraints of our experimental technique, however, tunneling is difficult to prove rigorously. In contrast to its protio analogue *o*-(trideuteriomethyl)phenylmethylene (**13b**) is thermally stable at 19 K; at higher temperatures the matrix softens and the carbene dimerizes. We are therefore unable to accurately measure k_D .

(24) West, P. R.; Chapman, O. L.; LeRoux, J.-P. *J. Am. Chem. Soc.* **1982**, *104*, 1779–1782. McMahon, R. J.; Abelt, C. J.; Chapman, O. L.; Johnson, J. W.; Kreil, C. L.; LeRoux, J.-P.; Mooring, A. M.; West, P. R. *J. Am. Chem. Soc.*, in press.

(25) McMahon, R. J.; Chapman, O. L.; Hayes, R. A.; Hess, T. C.; Krimmer, H.-P. *J. Am. Chem. Soc.* **1985**, *107*, 7597–7606.

(26) Trozzolo, A. M. *Acc. Chem. Res.* **1968**, *1*, 329–335.

(27) Porter, G.; Strachan, E. *Spectrochim. Acta* **1958**, *12*, 299–304. Andrews, L.; Miller, J. H.; Keelan, B. W. *Chem. Phys. Lett.* **1980**, *71*, 207–210.

(28) Pacansky, J.; Dupuis, M. *J. Am. Chem. Soc.* **1982**, *104*, 415–421.

(29) Pacansky, J.; Coufal, H. *J. Chem. Phys.* **1980**, *72*, 5285–5286. Pacansky, J., personal communication.

(30) Bodor, N.; Dewar, M. J. S. *J. Am. Chem. Soc.* **1972**, *94*, 9103–9106.

(31) Bell, R. P. *The Tunnel Effect in Chemistry*; Chapman and Hall: New York, 1980.

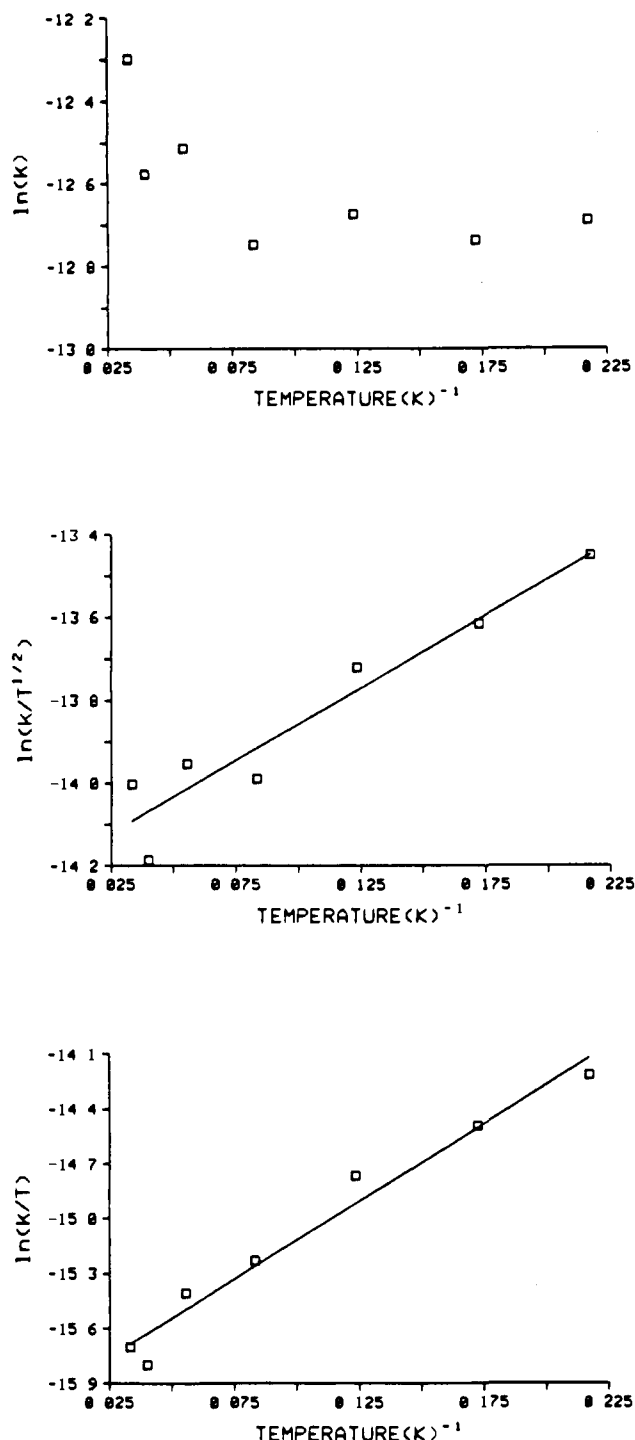


Figure 8. Temperature dependence of the rate of disappearance of the 249-nm UV absorption of *o*-tolylmethylene (**13a**) matrix isolated in argon. Top: Arrhenius theory. Middle: collision theory. Bottom: transition-state theory.

We can conservatively estimate a kinetic isotope effect (k_H/k_D) of at least 100. This value is not large enough to implicate tunneling, however. Because kinetic isotope effects depend on temperature, even a classical primary effect can be as large as 10^{12} at 20 K.³² Anomalous A_H/A_D values have been used to implicate tunneling,³¹ but we cannot measure A_D .

(32) A classical primary isotope effect arises due to the difference in zero-point energies (ZPE) of C-H and C-D stretching vibrations. To a first approximation, $\Delta ZPE = 2900 \text{ cm}^{-1}$ ($ZPE \nu_{C-H}$) - 2100 cm^{-1} ($ZPE \nu_{C-D}$) = 800 cm^{-1} = 1.15 kcal/mol. Assuming $\Delta ZPE = \Delta \Delta H = \Delta \Delta G$, we use the Eyring equation to calculate $k_H/k_D = \exp(-\Delta \Delta G/RT)$. At room temperature (298 K), we obtain the familiar results $k_H/k_D = 7$. However, at 65 K, $k_H/k_D = 7400$, and at 20 K, $k_H/k_D = 10^{12}$.

The theoretical basis for understanding both tunneling and the temperature dependence of hydrogen atom transfer reactions is still evolving.^{31,33-38} The different theories of reaction kinetics each predict a slightly different temperature-dependent rate behavior (eq 1-3).³⁹ In all three theories, the exponential term makes the dominant contribution to the temperature dependence of the rate constant at high absolute temperatures.³⁹ Under our cryogenic conditions, this need not be true; we must consider the possible temperature dependence of the pre-exponential factor. Arrhenius theory (eq 1) includes no temperature dependence in the pre-exponential factor, whereas collision theory (eq 2) includes a $T^{1/2}$ term and transition-state theory (eq 3) includes a T^1 term. McKinnon and Hurd have criticized the view of tunneling as a "correction" to classical behavior. They, and others, suggest an analysis in terms of eq 4.³⁴⁻³⁶ The Arrhenius plot for the thermal

$$k = A \exp(-E_a/RT) \quad (1)$$

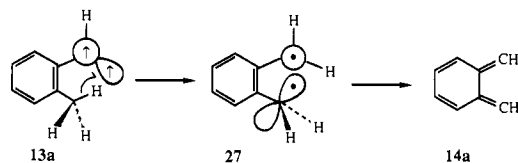
$$k = p d_{AB} [(8\pi kT/m_A m_B)(m_A + m_B)]^{1/2} \exp(-E^*/RT) \quad (2)$$

$$k = (\kappa T/h) \exp(\Delta S^\ddagger/R) \exp(-\Delta H^\ddagger/RT) \quad (3)$$

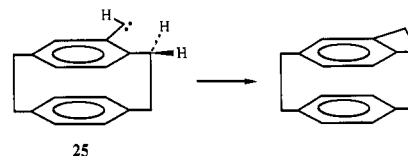
$$k = k_2 \exp(8m\pi^2 a^2 k_B T/h^2) \quad (4)$$

rearrangement of triplet *o*-tolylmethylene (**13a**) (Figure 8) deviates from linearity above ca. 20 K. This deviation may arise due to crossover between tunneling ("through the barrier") and classical ("over the barrier") behavior. Unfortunately, we cannot fully explore this possibility. Our temperature range is restricted to $T < 40$ K for argon matrices. In contrast to Arrhenius theory, the other "classical" theories accommodate the temperature-dependence data over the entire temperature range (Figure 8). The plot of $\ln(k)$ vs. T (eq 4) is no better than any of the classical plots (eq 1-3). This analysis failed at very low temperatures in other instances.³⁴

As tunneling reactions depend critically on distance,³¹ the best geometry results in transfer of an in-plane hydrogen atom to the carbene center in the anti rotomer of **13a**. The analogous reaction



of [2.2]-paracyclophanylmethylene (**25**) can occur only via transfer of an in-plane hydrogen atom.⁴⁰ The carbene center in **26** is locked in the orientation away from the alkyl group. In addition,



26 lacks the in-plane hydrogen atom. These facts explain the much higher thermal stability of **26**.⁶

We cannot distinguish between two possible mechanisms. The hydrogen migration may occur at the crossing of the triplet *o*-tolylmethylene surface with the singlet *o*-xylylene surface.⁴¹

(33) For an early review of proton transfer by tunneling, see: Caldin, E. F. *Chem. Rev.* **1969**, *69*, 135-156.

(34) LeRoy, R. J.; Murai, H.; Williams, F. J. *Am. Chem. Soc.* **1980**, *102*, 2325-2334.

(35) Siebrand, W.; Wildman, T. A.; Zgierski, M. Z. *J. Am. Chem. Soc.* **1984**, *106*, 4083-4089, 4089-4096.

(36) McKinnon, W. R.; Hurd, C. M. *J. Phys. Chem.* **1983**, *87*, 1283-1285.

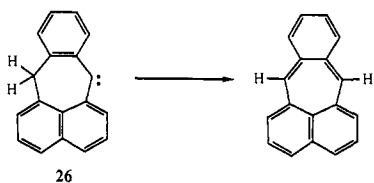
(37) Miyazaki, T.; Lee, K.-P.; Fueki, K.; Takeuchi, A. *J. Phys. Chem.* **1984**, *88*, 4959-4963.

(38) Dewar, M. J. S.; Merz, K. M.; Stewart, J. J. P. *J. Chem. Soc., Chem. Commun.* **1985**, 166-168.

(39) Carpenter, B. K. *Determination of Organic Reaction Mechanisms*; Wiley: New York, 1984; pp 123-124.

(40) Boxberger, M.; Volbracht, L.; Jones, M. *Tetrahedron Lett.* **1980**, 3669-3672.

(41) Griller, D.; Nazran, A. S.; Scaiano, J. C. *J. Am. Chem. Soc.* **1984**, *106*, 198-202.



Alternatively, tunneling may occur on the triplet surface to produce the twisted, triplet state of *o*-xylylene (**27**), which then internally converts to its ground state (**14a**).⁴² This pathway is thermodynamically feasible. Hehre measured the heat of formation of *o*-xylylene (**14a**) as 53 kcal/mol,⁴³ and theoretical calculations place the triplet biradical state of **14a** 22–26 kcal/mol above the singlet ground state.⁴⁴ Wentrup has estimated the heat of formation of triplet phenylmethylene as 102 kcal/mol.⁴⁵ This value represents a reasonable estimate for the heat of formation of triplet *o*-tolylmethylene (**13a**). It is thus clear that even the triplet excited state of **14a** lies well below the triplet ground state of **13a** (Figure 9).

The relationship between our results and Platz's studies of the *peri*-naphthylidiazomethanes⁶ is unclear. His failure to observe carbene **4a** is not necessarily surprising. Two factors make the hydrogen migration in 8-methyl-1-naphthylmethylene (**4a**) more favorable than that in *o*-tolylmethylene (**13a**). First, the distance between the methyl group and the carbene center is smaller in **4a** than in **13a**. Second, aromaticity is not destroyed by hydrogen migration in **4a**, as it is in **13a**. However, the failure to observe carbene **4b** suggests either facile deuterium atom tunneling in **4b** (an exciting prospect), migration in the excited state of the diazo compound, or photochemically induced migration caused by overirradiation of the carbene. The thermal deuterium shift contrasts with our observations in the *o*-tolylmethylene series and Iwamura's observations in the *o*-(9-fluorenyl)phenylnitrene series.⁸ In our system, we are able to specifically rule out migration in the excited diazo compound.

[1,2]-Hydrogen Shift in 1-Phenylethylidene (17a**)**. On a superficial level, one might expect to our study of 1-phenylethylidene (**17a**) to be strictly analogous to the closely related derivative (1,2-diphenylpropylidene (**1**)) studied by Tomioka and Platz.⁵ However, several important distinctions arise due to the different experimental conditions employed. First, Tomioka and Platz followed carbene disappearance by ESR spectroscopy. We observe the reaction by IR spectroscopy to be certain that we monitor the major processes occurring in the matrix. We observe both carbene **17a** disappearance and styrene (**18a**) appearance. Second, the extremely rigid polycrystalline host used by Tomioka and Platz causes the chemistry to display severe multiple site effect problems ($t^{1/3}$ decay). The methyl and phenyl substituents at C-2 severely restrict rotation in the rigid polycrystalline environment. In fact, Tomioka and Platz conclude that the chemistry of their singlet carbene "may be entirely predestined by the local matrix site, regardless of whether hydrogen or deuterium is α to the carbene center".^{5,7} In contrast to these problems, our xenon matrix is extremely soft at 65 K, as reflected by the first-order kinetics. Experiments described earlier suggest that the methyl group in **17a** rotates freely in argon at 15 K; it will certainly rotate freely in xenon at 65 K. The extremely slow deuterium shift in carbene **17b**, relative to the hydrogen shift in carbene **17a**, clearly rules out a matrix effect that predetermines the chemistry of our system. One of Tomioka and Platz's principle conclusions was "...solid-state ESR kinetic studies of unimolecular reactions of triplets will reveal more about environmental factors than about the desired reactions". The data depicted in Figure 5 demonstrate a "site clearing" effect. We simply suggest that, in this instance, the

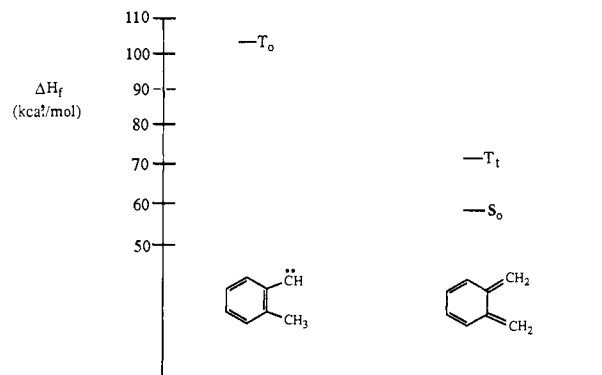


Figure 9. Heats of formation (ΔH_f) of *o*-tolylmethylene (**13a**) and *o*-xylylene (**14a**).

matrix effects are not severe enough to overwhelm the true intramolecular chemistry.

Yamamoto et al. concluded that conversion of 1-phenyldiazoethane (**16a**) to styrene (**18a**) occurs via a singlet excited state.⁴⁶ Numerous theoretical calculations of the [1,2]-hydrogen migration in CH_3CH predict small barriers (0–27 kcal/mol) for the S_1 reaction,^{1,29,47,48} but large barriers (20–88 kcal/mol) for the T_0 reaction.^{1,29,48,49} Thornton's experimental determination of a k_H/k_D value of 1.2–1.5 (at 298 K) implies a non-zero barrier to [1,2]-hydrogen migration.⁵⁰ Considerable theoretical and experimental evidence supports a reaction geometry in which the migrating C–H bond overlaps the vacant 2p orbital of the S_1 carbene.² Liu determined the barriers for [1,2]-hydrogen migration in ground-state-singlet (S_0) benzylbromocarbene (4.7 kcal/mol) and benzylchlorocarbene (6.4 kcal/mol).⁶²

Our results clearly demonstrate the existence of a barrier in the rearrangement of triplet 1-phenylethylidene (**17a**) to styrene. From the disappearance rate constant for **17a**, we use the Eyring equation to calculate $\Delta G^\ddagger_{65\text{K}} (\approx \Delta H^\ddagger \text{ at } 65 \text{ K}) = 4.7 \text{ kcal/mol}$. This value may reflect an external heavy-atom effect by xenon. The activation enthalpy is consistent with [1,2]-migration (either over or through the barrier⁵¹) in the thermally populated carbene S_1 state, but it is too small for T_0 reaction unless the theoretical calculations are grossly in error.^{1,29,47–49} This analysis fixes an upper limit of 4.7 kcal/mol on the T_0 – S_1 energy gap of **17a**. Other arylcarbenes display similar singlet–triplet splittings.^{52–54} We cannot exclude the possibility that the shift occurs by a surface-crossing mechanism.⁴¹

(46) For previous studies of 1-phenyldiazoethane chemistry, see: (a) Overberger, C. G.; Anselme, J.-P. *J. Org. Chem.* **1964**, *29*, 1188–1190. (b) Yamamoto, Y.; Murahashi, S.-I.; Moritani, I. *Tetrahedron* **1975**, *31*, 2663–2667; *Tetrahedron Lett.* **1968**, 5697–5701. (c) Moss, R. A.; Joyce, M. A. *J. Am. Chem. Soc.* **1977**, *99*, 1262–1264; 7399–7400.

(47) Raghavachari, K.; Frisch, M. J.; Pople, J. A.; Schleyer, P. v. R. *Chem. Phys. Lett.* **1982**, *85*, 145–149. Nobes, R. H.; Radom, L.; Rodwell, W. R. *Chem. Phys. Lett.* **1980**, *74*, 269–272.

(48) Altmann, J. A.; Csizmadia, I. G.; Yates, K. *J. Am. Chem. Soc.* **1974**, *96*, 4196–4201.

(49) Harding, L. B. *J. Am. Chem. Soc.* **1981**, *103*, 7469–7475. Rayez-Meume, M. T.; Decoret, C.; Dannenberg, J. J. *Chem. Phys. Lett.* **1978**, *55*, 431–434.

(50) Su, D. T. T.; Thornton, E. R. *J. Am. Chem. Soc.* **1978**, *100*, 1872–1875.

(51) Once again, we can conservatively estimate a kinetic isotope effect (k_H/k_D) of at least one or two orders of magnitude. This value is not large enough to implicate tunneling, however. Because of the temperature dependence of kinetic isotope effects, even a classical primary effect can be as large as 7400 at 65 K.³²

(52) Diphenylmethylene: T_0 – S_1 3, 3.9 \pm 0.2, 5.1 \pm 1 kcal/mol. Closs, G. L.; Rabinow, B. E. *J. Am. Chem. Soc.* **1976**, *98*, 8190–8198. DePuy, C.; Korenowski, G. M.; McAuliffe, M.; Heatherington, W. M.; Eisenthal, K. B. *Chem. Phys. Lett.* **1981**, *77*, 272–274. Eisenthal, K. B.; Turro, N. J.; Aikawa, M. A.; Butcher, J. A.; Du Puy, C.; Hefferon, G.; Heatherington, W. M.; Korenowski, E. M.; McAuliffe, M. J. *J. Am. Chem. Soc.* **1980**, *102*, 6563–6565.

(53) 9-Mesityl-9,10-dihydroboraanthrylidene: T_0 – S_1 > 5.2 kcal/mol. Lapin, S. C.; Brauer, B. E.; Schuster, G. B. *J. Am. Chem. Soc.* **1984**, *106*, 2092–2100.

(54) Phenylnitrene: T_0 – S_1 4.3 \pm 0.4 kcal/mol; T_0 – S_2 8.8 \pm 0.5 kcal/mol. Drzagic, P. S.; Brauman, J. I. *J. Am. Chem. Soc.* **1984**, *106*, 3443–3446.

(42) Efficient intersystem crossing occurs in 90°-twisted 1,4-biradicals. Salem, L.; Rowland, C. *Angew. Chem., Int. Ed. Engl.* **1972**, *11*, 92–111.

(43) Pollack, S. K.; Raine, B. C.; Hehre, W. J. *J. Am. Chem. Soc.* **1981**, *103*, 6308–6313.

(44) Dohnert, D.; Koutecky, J. *J. Am. Chem. Soc.* **1980**, *102*, 1789–1796. Maynaud, D.; Malrieu, J.-P. *J. Am. Chem. Soc.* **1982**, *104*, 3029–3034.

(45) Wentrup, C. *Tetrahedron* **1974**, *30*, 1301–1311.

Photophysics. Our study also yields information concerning the photophysical mechanism relating diazo compounds **12a** and **16a**, carbenes **13a** and **17a**, and hydrogen-migration products **14a** and **18a**. Our results clearly establish that photolysis of **12a** and **16a** produces the triplet carbenes **13a** and **17a**, respectively. Eisenthal's study of diphenyldiazomethane photochemistry indicates that triplet diphenylmethylene is formed from singlet diphenylmethylene by intersystem crossing.⁵⁵ If the same situation occurs in our system,⁵⁶ we must conclude that intersystem crossing of the initially formed singlet carbenes is faster than intramolecular hydrogen migration.⁵⁷ This contrasts with Iwamura's conclusions concerning the chemistry depicted in Scheme II.⁸

Photochemically initiated hydrogen migration in triplet carbenes **13a** or **17a** occurs upon T_0 - T_1 excitation (58 kcal/mol). If intersystem crossing of S_1 carbene to T_0 carbene is indeed fast (vide supra), then S_1 carbene cannot be responsible for hydrogen migration. This implies that an upper excited state (T_1 , S_2 , S_3) carbene also gives rise to hydrogen migration.

Summary. We examined intramolecular hydrogen shifts in carbenes by a variety of spectroscopic methods. The thermal rearrangement of triplet *o*-tolylmethylene (**13a**) to singlet *o*-xylylene (**14a**) occurs at temperatures as low as 4.6 K. Deviation from Arrhenius behavior at low temperatures suggests a tunneling mechanism. The thermal rearrangement of triplet 1-phenylethylidene (**17a**) to styrene (**18a**) likely occurs upon thermal population of the S_1 state of **17a** at 65 K.

Experimental Section

¹H NMR spectra were recorded on a Varian T-60 instrument. Chemical shifts (δ) are reported as ppm downfield from internal SiMe₄. Melting points were determined on a Thomas-Hoover Unimelt apparatus in open capillaries and are uncorrected. Elemental analyses were performed by Spang Microanalytical Laboratory (Eagle Harbor, MI). Mass spectra were obtained on AEI MS-9 or MS-902 spectrometers.

Infrared studies employed a Perkin-Elmer 580B spectrometer with a Model 3600 data station, or a Nicolet 60SX FTIR instrument. Ultraviolet-visible spectroscopy used a Perkin-Elmer 330 spectrometer with a Model 3600 data station. ESR spectra were obtained with an X-band spectrometer constructed from standard commercial components. The magnetic field was calibrated with an NMR gaussmeter, and the microwave frequency was determined by the use of a DPPH reference. The best fit of the observed ESR spectra with the spin Hamiltonian⁵⁸ (assuming $g_x = g_y = g_z = g_e$) provided the zero-field splitting parameters.

Matrix-Isolation Spectroscopy. The apparatus and experimental technique used for the study of reactive species matrix isolated in argon at 10 K have been described elsewhere.²⁵ The use of xenon necessitates some changes. At deposition temperatures below ca. 55 K, xenon forms a highly scattering, crystalline matrix, rather than an optically transparent glass. The sample window of our cryostat can be adjusted between 10 and 350 K; the protective inner shroud always remains at 40 K. With the window temperature set above 55 K, much of the xenon deposits on the colder inner shroud. We circumvented this problem by cutting off the portion of the inner shroud that surrounds the sample window. Even with this modified inner shroud, the window temperature remained below 15 K during irradiation. The vapor pressure of xenon is appreciable under high vacuum (10^{-6} Torr) at the temperatures employed during the deposition (55–65 K) and during the warming experiments (65–80 K). In order to minimize matrix degradation due to sublimation, only the forepump vacuum (10^{-3} Torr) was used at elevated temperatures.

UV-visible experiments below 10 K utilized an Air Products, Inc. Model LT-3-110A "Helitran" liquid helium transfer system. The sample was deposited on a sapphire window in the usual manner.²⁵ The cryostat was aligned in the spectrometer, and a spectrum of the starting material was recorded. After irradiation of the matrix, the cryostat was realigned in the spectrometer, and data acquisition was begun. The spectrometer's monochromator was set at 700 nm (0.1-nm slit) between scans to ensure that the instrument itself did not induce photochemistry in the matrix.

Sample Preparation. General procedures for syntheses of the tosylhydrazones, tosylhydrazone sodium salts, and diazo compounds used in this study are described elsewhere.²⁴

***o*-Tolualdehyde tosylhydrazone** was prepared from *o*-tolualdehyde (Aldrich) in 81% yield: mp 139–141 °C (lit.⁵⁹ mp 143–144 °C); ¹H NMR (CDCl₃) δ 2.30 (s, 3 H), 2.34 (s, 3 H), 7.05–7.75 (m, 6 H), 7.88 (AB, 2 H, $J = 8$ Hz), 8.06 (s, 1 H), 8.59 (br s, 1 H); Anal. (C₁₅H₁₆N₂O₂S) C, H, N.

***o*-Tolyldiazomethane (12a):** IR (Ar, 15 K) 3220 w, 3160 w, 3110 w, 3080 w, 3060 w, 3035 w, 2980 w, 2960 w, 2925 w, 2870 w, 2070 s, 1608 m, 1603 m, 1579 m, 1497 s, 1472 m, 1445 w, 1379 s, 1302 w, 1289 w, 1230 m, 1099 w, 1054 w, 1038 w, 790 w, 750 s, 715 w, 632 m, 546 w, 460 w, 425 m cm⁻¹; UV (Ar, 10 K) λ_{max} 500 br sh, 307, 294, 280, 275, 225, 219, 215 sh nm. The deep-red diazo compound was sublimed at -29 °C (10^{-6} Torr) and codeposited with argon to form a matrix.

***o*-(Trideuteriomethyl)benzaldehyde.** Morpholine (0.43 g, 4.86 mmol, 1.2 equiv; Baker) was dissolved in 10 mL of dry THF, cooled to -41 °C, and treated with 2.4 M *n*-BuLi-hexane (2 mL, 4.86 mmol).⁶⁰ After the mixture was stirred 5 min, 0.75 g of *o*-bromobenzaldehyde (4.05 mmol, 1.0 equiv; Aldrich) in 10 mL of dry THF was added dropwise via syringe over 2 min. The reaction was stirred for 15 min and then cooled to -78 °C. After the protected aldehyde was treated with 2.4 M *n*-BuLi-hexane (2.7 mL, 6.48 mmol, 1.6 equiv) dropwise over 7 min, 5 g of CD₃I (34.5 mmol, 8.5 equiv; Aldrich) was added, and the mixture was stirred at -78 °C for 1 h. The solution was warmed to room temperature, poured into 50 mL of 6 N HCl to deprotect the aldehyde, and extracted with Et₂O (4 \times 25 mL). The organic layers were washed with saturated aqueous NaHCO₃ (1 \times 25 mL) and saturated aqueous NaCl (1 \times 25 mL), dried over MgSO₄, and filtered. Removal of the solvent at reduced pressure afforded a dark brown liquid. Purification by column chromatography (SiO₂, Et₂O) yielded *o*-(trideuteriomethyl)benzaldehyde as a light yellow liquid (0.3 g, 60%). ¹H NMR (CDCl₃) δ 7.0–8.0 (m, 4 H), 10.0 (s, 1 H); IR (neat) 2735 m (aldehyde ν_{C-H}), 2220 w, 2125 w, 2055 w (trideuteriomethyl ν_{C-D}), 1695 s ($\nu_{C=O}$); mass spectrum (16 eV) m/z (relative intensity) 123 (M⁺, 41), 122 (22), 94 (18).

***o*-(Trideuteriomethyl)benzaldehyde tosylhydrazone** was prepared from *o*-(trideuteriomethyl)benzaldehyde in 51% yield: mp 139–142 °C; ¹H NMR (CDCl₃/Me₂SO-*d*₆) δ 2.37 (s, 3 H), 7.0–8.0 (m, 8 H), 8.12 (s, 1 H) (N-H not observed—sample slightly wet); mass spectrum (70 eV) m/z (relative intensity) 291 (M⁺, 22), 136 (42), 135 (38), 124 (33), 107 (76), 92 (52), 91 (100); high-resolution mass spectrum, calcd for C₁₅H₁₃D₃N₂O₂S 291.1121, found 291.1119. Anal. (C₁₅H₁₃D₃N₂O₂S) C, N, S.

***o*-(Trideuteriomethyl)phenyldiazomethane (12b):** IR (Ar, 15 K) 3115 w, 3080 w, 3035 w, 2235 w, 2070 s, 1603 s, 1495 s, 1453 m, 1388 m, 1382 m, 1296 w, 1238 w, 1055 w, 749 s, 691 w, 646 w, 632 m, 450 w, 440 vw, 423 w cm⁻¹; UV (Ar, 15 K) λ_{max} 480 br sh, 307, 301 sh, 299, 294, 278, 217 nm. The deep-red diazo compound was sublimed at -29 °C (10^{-6} Torr) and codeposited with argon to form a matrix.

Acetophenone tosylhydrazone was prepared from acetophenone (Eastman) in 80% yield: mp 133–135 °C; ¹H NMR (CDCl₃/Me₂SO-*d*₆) δ 2.22 (s, 3 H), 2.42 (s, 3 H), 7.2–8.2 (m, 9 H), 10.4 (s, 1 H); mass spectrum (16 eV) m/z (relative intensity) 288 (M⁺, 16), 133 (100), 132 (28), 105 (10), 104 (96), 92 (30), 91 (12). Anal. (C₁₅H₁₆N₂O₂S) C, H, N, S.

1-Phenyldiazoethane (16a): IR (Ar, 15 K) 3115 w, 3095 w, 3068 w, 3035 w, 3005 w, 2980 w, 2950 w, 2925 w, 2900 w, 2865 w, 2050 s, 1603 s, 1580 m, 1505 s, 1487 m, 1470 m, 1452 m, 1440 m, 1387 m, 1348 s, 1338 m, 1317 w, 1272 w, 1268 w, 1190 m, 1080 s, 1031 m, 999 w, 948 w, 888 w, 750 s, 718 w, 691 s, 635 m, 512 w, 482 m cm⁻¹; UV (Ar, 15 K) λ_{max} tail out to 580 nm, 315, 301 sh, 299 sh, 280, 243, 232, 224, 220 nm. The deep-red diazo compound was sublimed at -23 °C (10^{-6} Torr) and codeposited with argon to form a matrix.

α,α,α -Trideuterioacetophenone tosylhydrazone was prepared from α,α,α -trideuterioacetophenone (Merck) in 95% yield: mp 141–143 °C dec; ¹H NMR (CDCl₃/Me₂SO-*d*₆) δ 2.40 (s, 3 H), 7.2–8.0 (m, 9 H), 10.24 (s, 1 H); mass spectrum (16 eV) m/z (relative intensity) 291 (M⁺, 21), 140 (12), 137 (14), 136 (72), 135 (72), 134 (14), 107 (100), 106 (24); high-resolution mass spectrum, calcd for C₁₅H₁₃D₃N₂O₂S 291.1121, found 291.1111. Anal. (C₁₅H₁₃D₃N₂O₂S) C, N, S.

2,2,2-Trideuterio-1-phenyldiazoethane (16b): IR (Ar, 15 K) 3110 w, 3088 w, 3063 w, 3035 w, 2210 w, 2138 w, 2128 w, 2050 s, 1601 s, 1575 w, 1503 s, 1380 w, 1355 m, 1351 m, 1341 m, 1332 m, 1268 w, 1189 w,

(55) Eisenthal, K. B.; Turro, N. J.; Sitzmann, E. V.; Gould, I. R.; Hefner, G.; Langan, J.; Cha, Y. *Tetrahedron* **1985**, *41*, 1543–1554 and references therein.

(56) Admittedly, extrapolation from fluid solution at room temperature to an argon matrix at 10 K is dangerous.

(57) Intersystem crossing can be rapid at low temperatures. Photolysis of diphenyldiazomethane at 1.2 K produced triplet diphenylmethylene within the 8 ns laser pulse. Doetschman, D. C. *J. Phys. Chem.* **1976**, *80*, 2167–2169.

(58) Wasserman, E.; Snyder, L. C.; Yager, W. A. *J. Chem. Phys.* **1964**, *41*, 1763–1772.

(59) Nozaki, H.; Noyori, R.; Sisido, K. *Tetrahedron* **1964**, *20*, 1125–1132.

(60) Sinhababu, A. K.; Borchardt, R. T. *J. Org. Chem.* **1983**, *48*, 2356–2360.

(61) Regitz, M. *Chem. Ber.* **1965**, *98*, 1210–1224.

(62) Liu, M. T. H.; Subramanian, R. *J. Phys. Chem.* **1986**, *90*, 75–78. Liu, M. T. H. *J. Chem. Soc., Chem. Commun.* **1985**, 982–984.

1098 m, 1080 w, 1059 m, 993 w, 984 w, 889 w, 788 w, 747 s, 701 m, 690 m, 608 m, 508 w, 481 m cm^{-1} ; UV (Ar, 15 K) λ_{max} 500, 312, 302, 298 sh, 280, 245, 235, 228, 222 nm. The deep-red diazo compound was sublimed at -23°C (10^{-6} Torr) and codeposited with argon to form a matrix.

***p*-Methoxyacetophenone tosylhydrazone** was prepared from *p*-methoxyacetophenone (Aldrich) in 89% yield: mp $166\text{--}168^\circ\text{C}$ dec; $^1\text{H NMR}$ ($\text{CDCl}_3/\text{Me}_2\text{SO}-d_6$) δ 2.17 (s, 3 H), 2.38 (s, 3 H), 3.75 (s, 3 H), 6.82 (AB, 2 H, $J = 9$ Hz), 7.30 (AB, 2 H, $J = 8$ Hz), 7.54 (AB, 2 H, $J = 9$ Hz), 7.82 (AB, 2 H, $J = 8$ Hz), 10.23 (s, 1 H); mass spectrum (16 eV), m/z (relative intensity) 318 (M^+ , 11), 164 (9), 163 (100), 134 (45), 92 (10), 91 (14). Anal. ($\text{C}_{16}\text{H}_{18}\text{N}_2\text{O}_3\text{S}$) C, H, N.

1-(4-Methoxyphenyl)diazoethane (22). Preparation of the diazo compound in the usual manner produced a substantial amount of *p*-methoxystyrene (**24**) as a contaminant. IR (Ar, 15 K) 2055 s, 1272 s, 1188 s, 1082 w, 1049 s, 823 s, 805 m, 673 w, 614 m, 524 m, 482 w cm^{-1} . The deep-red diazo compound was sublimed at 0°C (10^{-6} Torr) and codeposited with argon to form a matrix.

1-Diazo-1-phenyl-2-propanone (21) was prepared by the method of Regitz.⁶¹ IR (Ar, 15 K) 2098 m, 2070 vs, 1679 s, 1660 w, 1611 w, 1503 m, 1369 s, 1331 m, 1290 m, 1245 s, 1148 w, 1036 m, 1008 w, 908 m,

752 s, 691 m, 618 m, 494 w cm^{-1} . The sample was sublimed at 8°C (10^{-6} Torr) and codeposited with argon to form a matrix.

Acknowledgment. We gratefully acknowledge the financial support of the National Science Foundation (Grant CHE84-04949) and the National Institutes of Health (Grant GM-24427). The National Science Foundation (1980-1983) and the IBM Corporation (1983-1984) provided predoctoral fellowships (R. J.M.). The National Science Foundation, the National Institutes of Health, the IBM Corp., and the Mobil Corp. supplied funds for the purchase of the Nicolet 60SX FTIR spectrometer.

Registry No. **12a**, 698-20-4; **12b**, 105930-64-1; **13a**, 35745-45-0; **16a**, 22293-10-3; **16b**, 105930-66-3; **17a**, 6393-09-5; **21**, 3893-35-4; **22**, 70078-14-7; D_2 , 7782-39-0; *o*-tolualdehyde tosylhydrazone, 35629-84-6; *o*-(trideuteriomethyl)benzaldehyde, 77765-22-1; *o*-(trideuteriomethyl)-benzaldehyde tosylhydrazone, 105930-63-0; α,α,α -trideuterioacetophenone tosylhydrazone, 105930-65-2; *p*-methoxyacetophenone tosylhydrazone, 32117-52-5; *o*-bromobenzaldehyde, 6630-33-7; acetophenone tosylhydrazone, 4545-21-5.

σ and π Interactions of the Carbonyl Ligand Determined from Single-Crystal Polarized Electronic Spectroscopy and Ligand Field Theory

Tsu-Hsin Chang and Jeffrey I. Zink*

Contribution from the Department of Chemistry and Biochemistry, University of California, Los Angeles, Los Angeles, California 90024. Received August 18, 1986

Abstract: The single-crystal polarized electronic absorption spectra of $(\text{Pr}_4\text{N})[\text{PtCl}_3\text{CO}]$, $(\text{Pr}_4\text{N})[\text{PtBr}_3\text{CO}]$, and $(\text{Pr}_4\text{N})[\text{PtCl}_3\text{CNC}(\text{CH}_3)_3]$ taken at 10 K are reported. Spin-allowed and spin-forbidden ligand field (d-d) transitions and charge-transfer transitions are assigned. The σ and π interactions of the carbonyl ligand with the metal d orbitals are obtained from full-matrix angular overlap ligand field theory calculations including spin-orbit coupling. The AOM σ and π parameters show that carbon monoxide is a very strong π acceptor ligand and that it is a good σ donor ligand. The σ and π interaction parameters are compared to those of other ligands of interest in organometallic chemistry, and the position of the carbonyl ligand in the two-dimensional spectrochemical series is reported. These comparisons show that carbon monoxide is a better σ donor ligand than the chloride ion and about equal to ethylene. The properties of the isonitrile ligand are similar to those of the carbonyl ligand. Bond length changes in excited electronic states determined from Franck-Condon analysis of the vibronic structure are reported.

The relative σ and π bonding properties of carbon monoxide in transition-metal complexes have been the subject of many experimental and theoretical studies. The importance of π back-bonding is firmly embedded in inorganic lore and is well documented in standard textbooks.¹ The σ -bonding properties, however, are not well documented.

The experimental measurement which is most amenable to theoretical interpretation and which has yielded the most insight into the bonding properties is IR spectroscopy. The standard lists of π -acceptor ligand series have been determined from trends in the CO stretching frequencies or from Cotton-Kraihanzel force constants.^{1,2} Extensions of this type of analysis have led to the development of series based on both σ and π effects.³ The general conclusion is that carbon monoxide is one of the best π -acceptor ligands but a poor σ donor. Other researchers have argued that there has been an overemphasis on π effects and that both σ and

π interactions must be considered.^{4,5}

Another experimental method of determining σ and π interactions of ligands with transition metals is electronic absorption spectroscopy. The σ and π interactions can be determined from transition energies and interpreted by using the angular overlap theory.⁶ However, such studies have been inhibited by three factors. First, the d-d transitions in complexes containing the carbonyl ligand are usually high in energy (as expected from a strong π -acceptor ligand). Second, intense charge-transfer bands, often in the same energy region as the d-d bands, obscure the weaker d-d bands which are needed for the analysis. Finally, the extinction coefficients are frequently large, thus preventing single-crystal polarized absorption spectra and hence resolved absorption bands from being obtained. A series of compounds in which the above problems can be overcome is the PtCl_3L^- series where L can range from Werner ligands⁷⁻¹⁵ to olefins,¹⁶ phosphines,

(1) Cotton, F. A.; Wilkinson, G. W. *Advanced Inorganic Chemistry*, 4th ed.; Wiley: New York, 1980; p 1078. Huheey, J. E. *Inorganic Chemistry*, 3rd ed.; Harper and Row: Cambridge, 1983; pp 432-441. Purcell, K.; Kotz, J. c. *Inorganic Chemistry*, Saunders, Philadelphia, 1977; p 201.

(2) Cotton, F. A.; Kraihanzel, C. S. *J. Am. Chem. Soc.* **1962**, *84*, 4432.

(3) Graham, W. A. G. *Inorg. Chem.* **1968**, *7*, 315.

(4) Angelici, R. J.; Ingemanson, C. M. *Inorg. Chem.* **1969**, *8*, 83.

(5) Brown, T. L.; Darenbourg, D. J. *Inorg. Chem.* **1968**, *7*, 959.

(6) Schaffer, C. E.; Jorgensen, C. K. *Mol. Phys.* **1965**, *9*, 401. Schaffer, C. E. *Struct. Bonding* **1968**, *5*, 68.

(7) Fenske, R. F.; Martin, D. S.; Ruedenberg, K. *Inorg. Chem.* **1962**, *1*, 441.